

## Time Resolved Pattern Evolution in a Large Aperture Laser

F. Encinas-Sanz, I. Leyva, and J. M. Guerra

*Departamento de Optica, Facultad de CC. Físicas, Universidad Complutense de Madrid, 28040 Madrid, Spain*  
(Received 2 July 1999; revised manuscript received 28 September 1999)

We have measured quasiinstantaneous transverse patterns in a broad aperture laser. Nonordered patterns yielding to boundary determined regular structures in progressive time-integrated recording are observed. The linear analysis and numerical integration of the full Maxwell-Bloch equations allow us to interpret the features of the experiment. We show that this system being far from threshold cannot be fully understood with a perturbative model.

PACS numbers: 42.65.Sf, 42.60.Jf, 42.60.Mi, 47.54.+r

Pattern formation in systems which exhibit spatiotemporal chaos has been a field of intense research in the last few years. An averaging process from chaotic to boundary-selected ordered patterns has been observed in hydrodynamics [1,2]. A similar behavior is foreseeable in other pattern forming systems, such as large aperture lasers.

In fact, this phenomenon has been predicted for lasers from the basis of the Maxwell-Bloch equations [3–5]. However, due to its extremely fast evolution, the time resolved spatiotemporal dynamics of a broad area laser has never been observed. So far, the experimental work only analyzes averaged patterns, mainly in cw CO<sub>2</sub> [3,6–8] and semiconductor lasers [9], since the minimum reachable exposure time was about 1  $\mu$ s, too long to obtain information about the pattern history.

In this Letter we study, both experimentally and theoretically, the time resolved dynamics of a large Fresnel number pulsed laser. The measurements were carried out with a system that we have recently developed to obtain infrared snapshots with a short exposure time (minimum  $\approx$  1 ns). This setup has been described in detail in Ref. [10], and it allows us to record virtually instantaneous transverse intensity laser patterns.

The source was a transversely excited atmospheric (TEA) CO<sub>2</sub> laser, with Fresnel number  $\mathcal{F} = \frac{b^2}{\lambda L} \approx 10$ , where  $2b = 20$  mm is the laser aperture,  $L = 1$  m is the resonator length, and  $\lambda = 10.6 \times 10^{-6}$  m is the lasing wavelength. This laser emits about 15% of the output energy in a gain-switch pulse ( $\sim 70$  ns), followed by a long collisional transfer tail ( $\sim 2-3 \mu$ s) [11]. Being a pulsed laser, it offers interesting characteristics such as high pumping far from threshold and wider detuning, which allow the exploration of additional features of the class B laser behavior.

In order to study the dynamics of the system, we take snapshots all along the duration of the laser pulse. A sample of recorded patterns taken with a 6 ns temporal resolution at different times along the pulse is shown in Fig. 1. Note that all the instantaneous patterns are disordered and are nonreproducible from shot to shot (Figs. 1a, 1b, and 1c).

However, such irregular appearance masks some kind of regularity, since the averaged patterns integrated all along the pulse length are ordered and reproducible (Fig. 1d), having eight or nine rolls parallel to the almost flat laser electrodes. The transverse spatial period of those bands

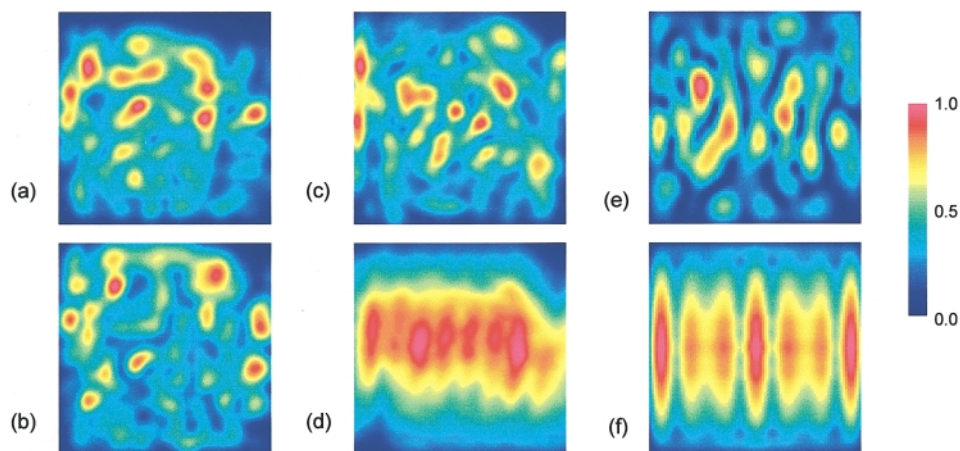


FIG. 1 (color). Instantaneous patterns at different times of the laser pulse. Experimental: (a) 150 ns, (b) 300 ns, and (c) 500 ns delay from the gain-switch pulse. Numerically generated: (e) 500 ns delay with  $Q_{\max} = 18.0$  and  $\delta = 0.6$ . Time-integrated patterns [experimental (d) and numerical (f)]. Experimental pattern dimension  $20 \times 20$  mm.

is  $\approx 1.8$  mm, similar to the size of the intensity maxima appearing in the disordered patterns. No sign of two spatial structure scales can be observed, contrary to the predictions of Ref. [3]. It is remarkable that the same regular structure is recovered by averaging over many equivalent instantaneous patterns, an observation that was suggested by the results in Ref. [12]. In this sense, a sort of ergodicity is observed.

We have also studied the temporal evolution of the intensity in one small area ( $\approx 1$  mm<sup>2</sup>), for which a photon-drag detector was used (rise time  $\approx 1$  ns). We find that the local intensity oscillates in a completely irregular form (Fig. 2a), with a period of 10 ns approximately. Furthermore, the cross correlation between the local oscillation measured at two different points of the patterns is very low, even if they are as close as 6 mm [13].

As the characteristic period of the intensity local fluctuations is about 10 ns, in order to record true instantaneous snapshots it would be convenient to reduce the width of the temporal window as much as possible below this value. But, if the window width is too small we do not get enough photons to be recorded by our system. On the other hand, a snapshot recorded with a much longer exposure integrates the pattern over several periods and it cannot be considered instantaneous any longer. That justifies the 6 ns choice that we have made for the temporal window width.

Nevertheless, it would be interesting to know how much recording integration time is necessary to obtain a sufficiently ordered pattern. Therefore, in order to follow the averaging process, we have also measured sequences of progressively integrated patterns by varying the temporal window (Fig. 3). These measurements were made in the first 150 ns of the laser pulse, in which the intensity is several times larger than in the pulse tail, and therefore the limitation due to the small intensity disappears. That allows us to reduce the time window down to 2 ns (Fig. 3a), showing a small number of intensity maxima which contrast deeply with the background. We see that the longer

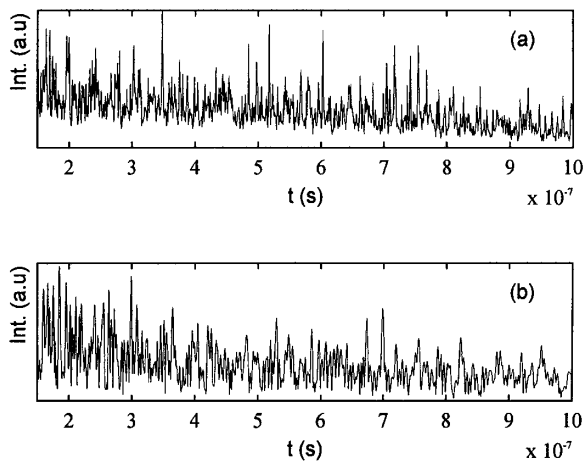


FIG. 2. Time evolution of the local intensity: (a) measured; (b) numerically generated for  $Q_{\max} = 18.0$ ,  $\delta = 0.6$ .

the exposure, the bigger the number of maxima observed (Figs. 3b and 3c), approaching progressively the ordered pattern, whose rolls are already clearly recognizable when the time integration is about 100 ns (Fig. 3d), yet much shorter than the total pulse duration.

Our theoretical approach to the problem includes both numerical simulations and a linear stability analysis of the full Maxwell-Bloch laser equations.

Hence, in order to reproduce the spatiotemporal dynamics, we directly integrate the two-level Maxwell-Bloch equations [4]:

$$\frac{\partial E}{\partial t} = -\kappa \left[ (1 - i\delta) - i \frac{a}{2} \Delta_t \right] E - \kappa Q P, \quad (1)$$

$$\frac{\partial P}{\partial t} = -\gamma_{\perp} [D E + (1 + i\delta) P], \quad (2)$$

$$\frac{\partial D}{\partial t} = -\gamma_{\parallel} \left[ D - 1 - \frac{1}{2} (E P^* + E^* P) \right], \quad (3)$$

where  $E = E(\mathbf{x}, t)$  is the slowly varying electric field,  $P = P(\mathbf{x}, t)$  is the polarization,  $D = D(\mathbf{x}, t)$  is the population inversion,  $Q = Q(\mathbf{x}, t)$  is the rescaled pump,  $\kappa = \frac{c}{2L} \ln(R)$  representing the cavity losses with  $R = \sqrt{R_1 R_2} = 0.78$  the resonator reflectivity,  $a = \frac{c}{2\kappa L \mathcal{F}}$  is a diffraction coefficient,  $\delta = \frac{\omega_{21} - \omega}{\gamma_{\perp}}$  is the rescaled detuning, and  $\Delta_t$  is the Laplacian in the adimensional transverse coordinates of the system  $\mathbf{x} = (x, y)$ . In an atmospheric laser, the decay rates can be chosen as  $\gamma_{\perp} = 3 \times 10^9$  s<sup>-1</sup>,  $\gamma_{\parallel} = 10^7$  s<sup>-1</sup>, and  $\kappa = 3.9 \times 10^7$  s<sup>-1</sup>.

The transversal pumping profile is taken to be homogeneously distributed along one transverse axis and Gaussian

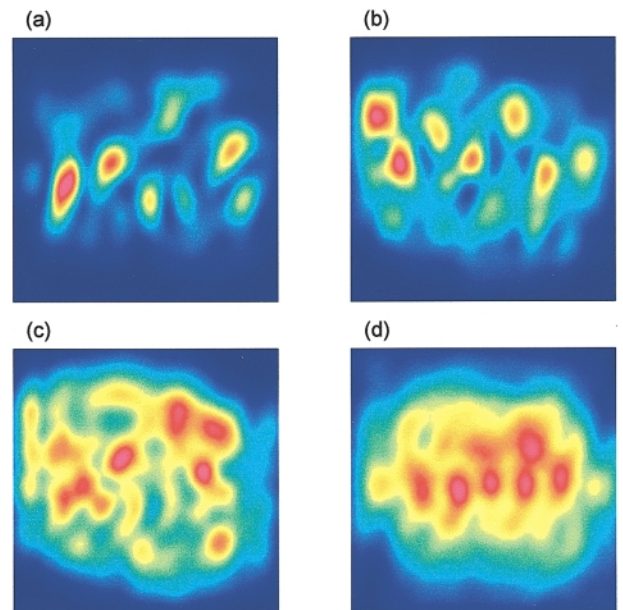


FIG. 3 (color). Experimental patterns with different exposure time: (a) 2 ns, (b) 6 ns, (c) 30 ns, and (d) 100 ns.

in the other, in order to reproduce the experimental current spatial distribution of the discharge. Likewise, the temporal form of the pumping was simulated by a function approximating the pulsed excitation, with typically large pumping parameters in the maximum ( $Q_{\max} \approx 15\text{--}25$ ). Null boundary conditions, equivalent to the experimental ones, were used.

The patterns and local intensity temporal evolution obtained by a standard numerical method look very similar to those recorded experimentally. In the spatial domain, the instantaneous patterns (Fig. 1e) are well reproduced, as well as the time integrated (Fig. 1f). In both of them, only one spatial scale of structures is found, in accordance with the experimental records. The numerical temporal evolution (Fig. 2b), although completely irregular, presents a characteristic time of the same order as its experimental counterpart (Fig. 2a).

As has been mentioned, this time scale of the irregular oscillations measured in the local dynamics is around a few nanoseconds (Fig. 2), whereas the typical evolution time of the pulsed pumping is a few microseconds ( $2\text{--}3 \mu\text{s}$ ). A good approximation is to consider the dynamics measured in the slow varying pulse tail to be quasistationary [14]. Thus, we can still use the properties of a linear stability analysis to gain some deeper insight into the observed irregular dynamics. Taking this consideration into account, we undertake the stability study linearizing Eqs. (1)–(3). As is known, the Liapunov exponents of the equations are the real parts of the five roots of the corresponding secular quintic equation, which cannot be solved analytically, and therefore it is not possible to obtain algebraic expressions for the eigenvalues. However, it is known that, for class B lasers, out of the five roots, one is real and the rest come in complex conjugated pairs [4,6].

It can be shown that the resonator can develop the instability associated to the real root only when the condition

$$\delta \frac{Q - (1 + \delta^2)}{Q} \gg \frac{-\pi}{4\mathcal{F} \ln(R)} \quad (4)$$

is satisfied [4]. In a TEA-CO<sub>2</sub> laser, only one molecular transition oscillates (P20 line, Ref. [15]). In the present case, it includes a large number of axial modes simultaneously (15–20), with a free spectral range of  $\frac{c}{2L} \approx 150$  MHz [13]. Hence, most of the values of  $\delta$  lie in the interval  $-1 \leq \delta \leq 1$ . Since  $Q \gg 1$ , the condition (4) is not satisfied for most of the oscillating axial modes. Thus, we conclude that this instability does not actually affect the laser, or does so very weakly.

In addition, two of the complex conjugate roots can be approximated as  $-\gamma_{\perp}(1 \pm i\delta)$ , being their real part always negative and therefore not associated to any instability.

The detuning value determines whether the real parts of the two remaining conjugate roots are negative for every transverse wave-vector  $k$ , or positive for an interval around a value  $k_o(\delta)$ , the wavelength vector at which the Liapunov

exponent is maximum and positive (Fig. 4). Each set of system parameters has a certain critical detuning  $\delta_c$ ; such as for  $\delta > \delta_c$ , there is an interval of wave numbers  $k$  for which the real part of the root is positive. In the present case this critical value is rather low ( $\delta_c \sim 0.06$ ). Then, for most of the axial modes with  $\delta > 0$ , the instability associated to those complex conjugate roots shows up.

Summarizing, in this kind of laser most of the axial modes with positive detuning bear the short-wavelength instability due to the pair of complex conjugate roots, whereas that associated to the real root is not supported because of the diffraction (Fig. 4). Therefore, the observed irregular spatiotemporal behavior can be justified only by the action of the remaining instability, in contrast with [6].

On this basis, it is possible to estimate the expected spatial and temporal scales. The spatial scale of the instabilities associated to the complex root will be around  $k_o^{-1}$ . By solving numerically the secular equation with  $\delta = 0.6$  and  $Q = 6.0$  (a reasonable mean value in the pulse tail), we obtain  $k_o = 3225 \text{ m}^{-1}$ . Then the size of the generated structures should be

$$S_0 = 2\pi k_o^{-1} \approx 1.94 \times 10^{-3} \text{ m}. \quad (5)$$

The average size of the experimentally measured intensity maxima in the instantaneous patterns and, consequently, the spatial period of the bands appearing in the time integrated patterns is

$$S_{\text{exp}} = 1.8 \times 10^{-3} \text{ m}. \quad (6)$$

The agreement between (5) and (6) relates the observed dynamics with the remaining instability.

Furthermore, the imaginary part of these eigenvalues gives the oscillation frequency of the solutions. Hence, for the same  $k_o$ , we obtain  $\omega \approx 360 \times 10^6 \text{ s}^{-1}$ , corresponding to a period of 16 ns, very close to both the experimental and the numerically obtained fluctuation period of  $\sim 10$  ns (Figs. 2a and 2b). Thus, the time scale is also well predicted by the stability analysis.

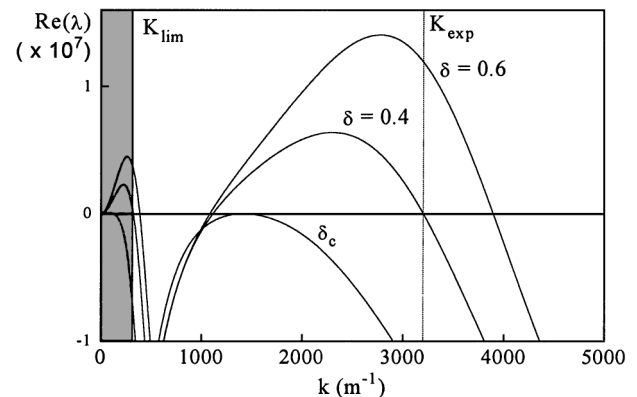


FIG. 4. Real ( $\lambda$ ) for several  $\delta$  values,  $K_{\text{lim}}$  being the diffraction limit for the instabilities, and  $K_{\text{exp}}$  the experimentally found mean wave number.

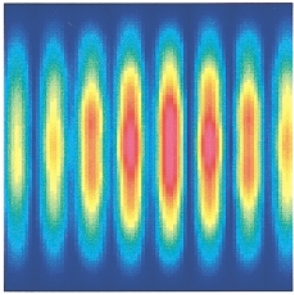


FIG. 5 (color). Numerically generated instantaneous pattern for  $Q_{\max} = 2.0$ ,  $\delta = 0.6$ .

Concerning the physical interpretation of the irregular observed dynamics, in the present case the suppression of the instability coming from the real root invalidates its being considered as the origin of the disordered instantaneous pattern. Thus we found that even though the distance to the threshold is moderate here ( $Q \sim 6$ ), an analysis based on the order parameter equation seems to already be insufficient. To test this, the same numerical integration has been carried out for a hypothetical case nearer threshold ( $Q_{\max} = 2$ ), where the order parameter equations must dominate the amplitude behavior [4]. In agreement with this perturbative approach, since the phase instability is inhibited here, the instantaneous patterns show a large degree of order (regular rolls which oscillate periodically; Fig. 5). However, in the far threshold pumping case they are disordered, and, therefore, the present problem does not seem suitable for reduction to a perturbative one, as is usual in the theoretical approaches. In other words, in the observed dynamic it is not possible to distinguish between phase and amplitude fluctuations. This result is a test of the validity range of the order parameter equations, which was not easily verified experimentally. As a more probable origin of the phenomenon, a secondary instability of the traveling wave solutions can be suggested [16].

In conclusion, in this Letter we report the measurement of time resolved intensity patterns in a large aperture laser, by means of an experimental system developed in our laboratory. A rich irregular intensity spatiotemporal dynamics, usually masked under time-integrated measurements, has been uncovered. We show experimental evidence of how this local irregular dynamics averages

to boundary determined order, as had been observed in other pattern forming systems but so far predicted only theoretically for lasers. Besides, a numerical integration of the two-level full Maxwell-Bloch equations and its corresponding stability analysis reproduces the experimental observations with outstanding agreement.

This work has been supported by DGICYT Project No. PB95-0389 (Spain).

- 
- [1] Li Ning, Yuchou Hu, R. E. Ecke, and G. Ahlers, *Phys. Rev. Lett.* **71**, 2216 (1993).
  - [2] B. J. Gluckman, P. Marcq, J. Bridger, and J. P. Gollub, *Phys. Rev. Lett.* **71**, 2034 (1993).
  - [3] G. Huyet, M. C. Martinoni, J. R. Tredicce, and S. Rica, *Phys. Rev. Lett.* **75**, 4027 (1995).
  - [4] G. Huyet and S. Rica, *Physica (Amsterdam)* **96D**, 215 (1996).
  - [5] K. Staliunas and C. O. Weiss, *J. Opt. Soc. Am. B* **12**, 1142 (1995).
  - [6] G. Huyet and J. R. Tredicce, *Physica (Amsterdam)* **96D**, 209 (1996).
  - [7] A. Labate, M. Ciofini, R. Meucci, S. Boccaletti, and F. T. Arecchi, *Phys. Rev. A* **56**, 2237 (1997).
  - [8] D. Dangoisse, D. Hennequin, C. Lepers, E. Louvergneaux, and P. Glorieux, *Phys. Rev. A* **46**, 5955 (1992).
  - [9] S. P. Hegarty, G. Huyet, J. G. McInerney, and K. D. Choquette, *Phys. Rev. Lett.* **82**, 1434 (1999).
  - [10] F. Encinas-Sanz, O. G. Calderon, R. Gutierrez-Castrejon, and J. M. Guerra, *Phys. Rev. A* **59**, 4764 (1999).
  - [11] F. Encinas-Sanz and J. M. Guerra, *IEEE J. Quantum Electron.* **27**, 891 (1991).
  - [12] F. Encinas-Sanz, J. M. Guerra, and I. Pastor, *Opt. Lett.* **21**, 1153 (1996).
  - [13] I. Pastor, F. Encinas-Sanz, and J. M. Guerra, *Appl. Phys. B* **52**, 184 (1991).
  - [14] D. J. Biswas and R. G. Harrison, *Opt. Commun.* **47**, 3 (1986).
  - [15] N. N. Vorobeve, M. G. Galushkin, E. P. Glotov, V. G. Lyakishev, V. I. Rodionov, A. M. Seregin, N. V. Cheburkin, and S. K. Chekin, *Sov. J. Quantum Electron.* **14**, 7 (1994).
  - [16] See, for instance, M. C. Cross and P. C. Hohenberg, *Rev. Mod. Phys.* **65**, 851 (1993); P. K. Jacobsen, J. Lega, Q. Feng, M. Stanley, J. V. Moloney, and A. C. Newell, *Phys. Rev. A* **49**, 4189 (1994).